ACS OMEGA

http://pubs.acs.org/journal/acsodf

Article

First Evidence of Pheomelanin-UVA-Driven Synthesis of Pummerer's Ketones by Peroxidase-Mediated Oxidative Coupling of Substituted Phenols

Sofia Gabellone,[‡] Eliana Capecchi, Lucrezia Anastasia Ortelli, and Raffaele Saladino*[,‡]

Cite This: *ACS Omega* 2022, 7, 45688−45696

Read Online

ACCESS | Metrics & More | Article Recommendations | Supporting Information

ABSTRACT: Photoexcitation of pheomelanin produces high-energy singlet oxygen and the superoxide anion, which are reactive species in damage of cellular targets. In principle, these species can be involved in processes of synthetic utility when adequate experimental conditions are defined. Here, we describe that pheomelanin performs as a selective UVA antenna for the horseradish peroxidase oxidative coupling of substituted phenols to biologically active Pummerer's ketones under 2-methyltetrahydrofuran/buffer biphasic conditions. In this system, singlet oxygen is scavenged by conversion of 2-methyltetrahydrofuran into the corresponding organic hydroperoxide, while the superoxide anion is dismutated into hydrogen peroxide. Both these intermediates are able to oxidize the active site of horseradish peroxidase triggering the oxidative coupling reaction. Trimer derivatives, produced by addition of phenoxy radicals on preformed Pummerer's ketones were also isolated, suggesting the possibility to further improve the structural complexity of the reaction products.

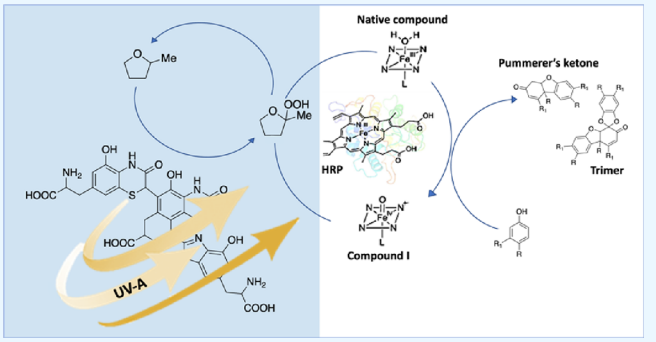

INTRODUCTION

Pheomelanin is a product of random polymerization of cysteinyl-dopa precursors via benzothiazole and benzothiazine intermediates.[1−4] It is commonly considered as a UVA photosensitizing agent in cellular damage,[5−7] as a consequence of the generation of singlet oxygen and the superoxide anion[8,9] and other radical centered oxygen species (ROS).[10−14] Alternatively, excited pheomelanin can be reduced by accepting electrons from biological reductants (e.g., NAD(*P*)H and glutathione) and organic substrates.[15,16] Examples of generation of singlet oxygen by pheomelanin at a higher value of wavelength than UVA are reported as in the case of blue-light photons albeit in a very low yield. In addition, pheomelanin is redox-active in dark conditions.[17] An important issue in challenging the application of pheomelanin in organic synthesis is the fate of singlet oxygen and the superoxide anion upon photoexcitation.[18,19] We recently reported that singlet oxygen generated by blue-LED irradiation of *meso*-tetraphenyl porphyrin (*meso*-TPP) is selectively trapped by 2-methyltetrahydrofuran (2-MeTHF) to produce the corresponding organic hydroperoxide in the activation of horseradish peroxidase (HRP).[20] This procedure avoided the inhibition of HRP by an excess of H_2O_2 under experimental conditions simpler than photochemical reduction of dioxygen by natural or synthetic cofactors.[21−24] Moreover, the superoxide anion is responsible for the transformation of the ferric heme-prosthetic group (native form of HRP) to inactive compound **III** (oxy-peroxidase), as well as for the transformation of active compound **I** (Fe(V) π−cation radical) to compound **II** (Fe(IV) ferryl intermediate), and of compound **II** to the native form. The spontaneous decomposition of compound **III** to the native form and the superoxide anion completes the cycle of interactions (Figure 1). In addition, the superoxide anion inhibits the HRP-mediated oxidative coupling of phenols by quenching phenoxyl radical intermediates. The detrimental effect of the superoxide anion can be counter balanced at acidic pH or in the presence of superoxide dismutase (SOD).[25,26] These conditions favor the dismutation of the superoxide anion to H_2O_2.[27] Thus, HRP can work in the presence of singlet oxygen and the superoxide anion only if favorable experimental conditions are operative, that is, the trapping of singlet oxygen by formation of organic hydroperoxides and the dismutation of the superoxide anion into H_2O_2. Is it really possible to use pheomelanin as a selective photosensitizing agent to drive photochemical UVA/HRP-mediated organic transformations in the presence of these reactive species? Here, we report the first evidence that biologically active Pummerer's

Received: October 12, 2022
Accepted: November 8, 2022
Published: November 29, 2022

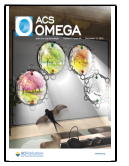

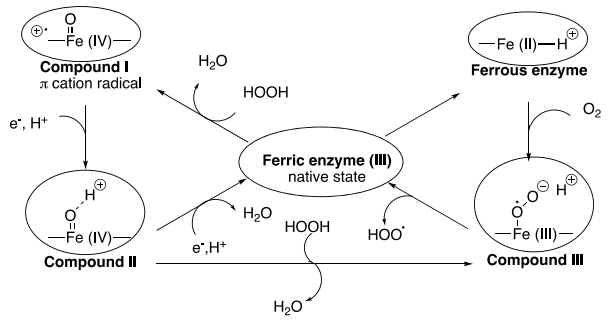

Figure 1. Catalytic cycle of peroxidase and the effect of the superoxide anion.

ketones, which represent synthons for different natural products, are synthesized by oxidative coupling of substituted phenols in a protective group-free procedure by pheomelanin-UVA-driven activation of HRP. In this study, 2-methyltetrahydrofuran (2-MeTHF) was used as a sustainable solvent to capture singlet oxygen, while the superoxide anion was contemporarily transformed to H_2O_2 under acidic conditions. We compared the photocatalytic efficiency of two synthetic pheomelanins synthesized from L-cysteine and L-Dopa by chemical oxidation with sodium permanganate (PM-K) or, in alternative, by mushroom tyrosinase enzymatic polymerization (PM-T).[28] The pheomelanin samples showed a different efficacy in the oxidative coupling of phenols probably due to their specific content of photoactive aromatic subunits. In particular, the synthesis of Pummerer's ketones was highly efficient and selective at pH 6 and room temperature in the presence of PM-K, with the yield of desired products being higher in biphasic conditions (2-MeTHF/buffer) than in the monophasic counterpart (2-MeTHF).

RESULTS AND DISCUSSION

Preparation of Pheomelanin Samples. PM-K and PM-T were synthesized starting from L-cysteine and L-Dopa by a modification of previously reported procedures[29,30] (experimental details are in Supporting Information S1 and S2, respectively). UV−vis analysis of samples (Figure S1) showed the absorption bands expected for pheomelanin. Field-emission scanning electron microscopy (FESEM) of PM-K confirmed the formation of spherical particles with an average diameter of 100 nm (Figure S2, panel A). Instead, PM-T showed particles with an irregular morphology (Figure S2, panel B). Energy-dispersive X-ray elemental analysis (EDX) quantified the incorporation of cysteine in the samples in the amounts of 15.46 and 6.56 wt % of sulfur atoms (Table S1; EDX of PM-K is in Figure S3). Electron paramagnetic resonance (EPR) spectra of PM-K were characterized by a "*g*" value of 2.004 in accordance with the literature (Figure S4, panel A).[31] Instead, the EPR signal of PM-T was not well-resolved (Figure S4, panel B). The UHPLC−MS analysis (Figure S5, panel A) of PM-K showed 4-methylthiazole as a repetitive fragment (*m*/*z* 100) typical of the benzothiazole subunit of pheomelanin, while the pyrrole fragment (*m*/*z* 68), associated to DHICA subunits of eumelanin, prevailed in the case PM-T (Figure S5, panel B). Finally, the C−S stretching vibration mode at 700−600 cm^{-1} was detected in the FT-IR analysis of both samples (Figure S6; panel A and panel B). Overall, PM-K was characterized by higher pheomelanin character than PM-T. These data were in accordance with the low content of aromatic subunits previously reported for PM-T with respect to PM-K.[28]

Synthesis of Pummerer's Ketones. The activity of HRP was initially evaluated by the pyrogallol assay in dark conditions and in the presence of PM-K and PM-T at pH 6 and pH 7, respectively.[32,33] As reported in Table 1 (entry 1 versus entries 4 and 6), the enzymatic activity was not significantly modified with respect to the reference (HRP alone) in the presence of pheomelanin samples at pH 7, while a slight decrease of the enzymatic activity was observed at pH 6, probably due to the occurrence of supramolecular interactions between HRP and pheomelanin (Table 1, entry 2 versus entries 5 and 7).[34,35] In a similar way, HRP retained the original activity after UVA irradiation at pH 7 for 24 h at 27 °C (Table 1, entry 3 versus entry 1).[36]

Table 1. Activity of HRP in the Presence of Pheomelanin Samples at Selected pH Values

entry	photosensitizer	pH	activity (U/mg)
1	none	7	126.1
2	none	6	90.2
3	none[a]	6	118.7
4	PM-K	7	132.1
5	PM-K	6	90
6	PM-T	7	122.6
7	PM-T	6	104.1

[a]Experiments were performed after UVA irradiation of HRP. All the reactions were conducted in triplicate.

We started our investigation analyzing the oxidation of *para*-cresol **1** in the presence of PM-K under biphasic conditions.[20] The schematic representation of the biphasic system is in Figure 2. It includes (i) the photoactivation of pheomelanin and intercrossing system decay to the triplet state and successive generation of singlet oxygen (pathway A); (ii) the formation of the organic hydroperoxide **I** by selective carbon-alpha insertion of singlet oxygen into the tertiary carbon atom of 2-Me-THF and diffusion of hydroperoxide **I** from the organic layer to the buffer (pathway B); (iii) the activation of HRP and successive oxidative radical coupling (pathway C). Briefly, compound **1** (108.1 mg, 1.0 mmol) dissolved in 2-MeTHF (5.0 mL) was added with PM-K (5 mg, 1.0% w/w with respect to the substrate) and HRP (17, 34 and, 68 units) in 5.0 mL of PBS (0.1 M, pH 7.0). The amount of PM-K was selected on the basis of data previously reported by us on the use of *meso*-tetraphenyl porphyrin (*meso*-TPP) and blue-led photons.[20] 2-MeTHF is a green and water-immiscible solvent deprived of any toxic effect.[37,38] The solution was gently stirred (200 rpm) at 27 °C for 48 h in an air atmosphere under UVA irradiation (365 nm). Irrespective of the experimental conditions, 4a,9b-dihydro-8,9b-dimethyl-3(4*H*)-dibenzofuranone **2** (Pummerer's ketone) was obtained as the main reaction product, in addition to 2,2′-dihydroxy-5,5′-dimethyldiphenyl **3** (*ortho*−*ortho* dimer) as a side product (Scheme 1 and Table 2, entry 1), highlighting the effective capacity of PM-K to act as a photosensitizer in the synthesis of the Pummerer's ketone.

Note that the reaction was ineffective in a dark reactor, under anaerobic conditions (argon atmosphere), and in the absence of HRP, as well as in the presence of alternative organic solvents lacking a tertiary C−H bond, such as petroleum ether or *n*-hexane (S3). Pummerer's ketone **2**

https://doi.org/10.1021/acsomega.2c06584
ACS Omega 2022, 7, 45688−45696

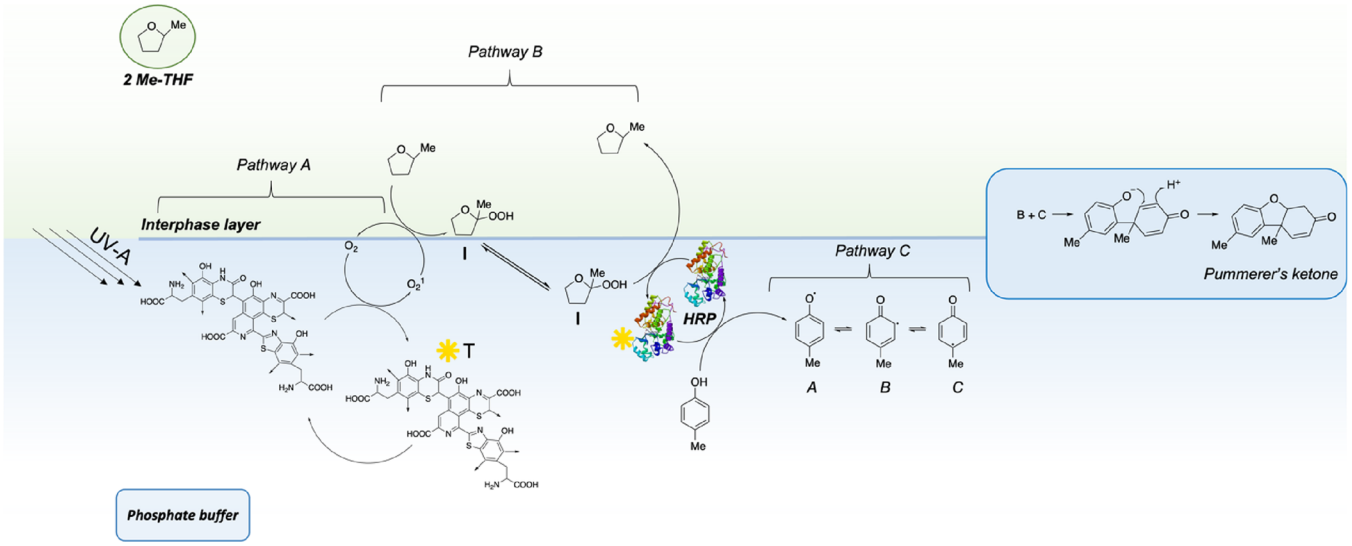

Figure 2. Schematic representation of the UVA-driven pheomelanin/HRP-mediated photobiocatalytic system: (i) photoactivation of pheomelanin and generation of singlet oxygen (pathway A); (ii) formation of hydroperoxide **I** and its diffusion to the buffer layer (pathway B); (iii) activation of HRP and successive oxidative radical coupling process involving mesomeric forms A, B, and C in the selected case of *para*-cresol **1** (pathway C).

Scheme 1. Synthesis of Pummerer's Ketone 2 and Dimers 3 and 4 by UVA-Driven Pheomelanin/HRP-Mediated Oxidative Coupling of *para*-Cresol 1 in Biphasic Conditions

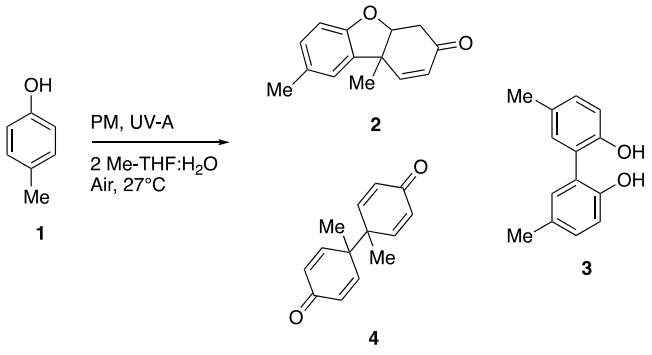

showed all the characteristic NMR signals expected for the tricyclic structure.[39] In particular, the presence of the H-4 hydrogen signal at 4.71 ppm (multiplet) coupled with the adjacent CH_2 group (double doublet centered at 3.05 ppm) confirmed the closure of the central tetrahydrofuran ring. In this latter case, the oxidative coupling proceeded by coupling of the *ortho*- and *para*-radical mesomeric forms of the substrate followed by internal Michael addition (Figure 2, panel A).[40] As an alternative, dimer **3** was derived from *ortho*−*ortho* oxidative coupling.[41] Compounds **2** and **3** were previously obtained by oxidation of compound **1** with HRP and an excess of H_2O_2 in a lower yield.[42] The effective formation of hydroperoxide **I** during UVA irradiation of PM-K was evaluated by the pyrogallol assay performed at pH 7 and pH 6 and at different reaction times (1, 4, 24, and 48 h).[32,33] As reported in Figure S7 (panel A), the concentration of hydroperoxide **I** increased by increasing the irradiation time, reaching the highest value after 48 h (47.5 and 49.4 μmol/mL, respectively). A similar trend was observed in the case of PM-T (Figure S7, panel B). Once formed, hydroperoxide **I** recognized the ferric heme (Fe(III)) of HRP by neighboring group participation of the endocyclic oxygen followed by delivery of the oxygen atom and regeneration of 2-MeTHF.[20,24] The reaction was repeated in the absence of HRP using coumarin as a selective OH scavenger ("coumarin assay") to exclude the formation of hydroxyl radicals ($OH^{\cdot}$).[43,44] No trace amounts of $OH^{\cdot}$ were detected in the reaction mixture confirming the concerted nature of the transfer of the oxygen atom in the formation of the hydroperoxide **I** (Figure S8).[45]

From the synthetic point of view, the Pummerer's ketone was obtained in the highest yield in the presence of 17 units of HRP (Table 2, entry 3 versus entries 1 and 2). The low mass balance observed in the presence of 68 units of HRP was probably due to the occurrence of oligomerization of

Table 2. Pheomelanin UVA-Driven HRP-Mediated Oxidative Coupling of *para*-Cresol 1 in Biphasic Conditions

entry	photosensitizer (amount % w/w)	pH	HRP (U/mg)	conversion (%)	product(s)	yield (%)[a]
1	PM-K (1.0%)	7	68	73	**2**(3)	30.1(5)
2	PM-K (1.0%)	7	34	70	**2**(3)	38.7(11)
3	PM-K (1.0%)	7	17	66	**2**(3)	41.8(16)
4	PM-K (1.0%)	6	17	76	**2**(3)[**4**]	50.7(16.3)[1.1]
5	PM-K (0.5%)	6	17	71	**2**(3)[**4**]	28.7(12)[1.6]
6	PM-K (0.25%)	6	17	49	**2**(3)	18.0(2.1)
7	PM-T (1.0%)	6	17	37	**2**(3)	34(4)
8	PM-T (0.5%)	6	17	23	**2**(3)	26.4(3)
9	PM-T (0.25%)	6	17	12	**2**(3)	22(2)

[a]Yield was calculated based on the amount of the converted substrate. All the reactions were conducted in triplicate.

https://doi.org/10.1021/acsomega.2c06584
ACS Omega 2022, 7, 45688−45696

Scheme 2. Synthesis of Pummerer's Ketones 5a and 6a, Spirobenzo[1,3]-dioxol Trimers 5c and 6c, and Related Dimers by UVA-Driven Pheomelanin/HRP-Mediated Oxidative Coupling of Phenol Derivatives 5−8

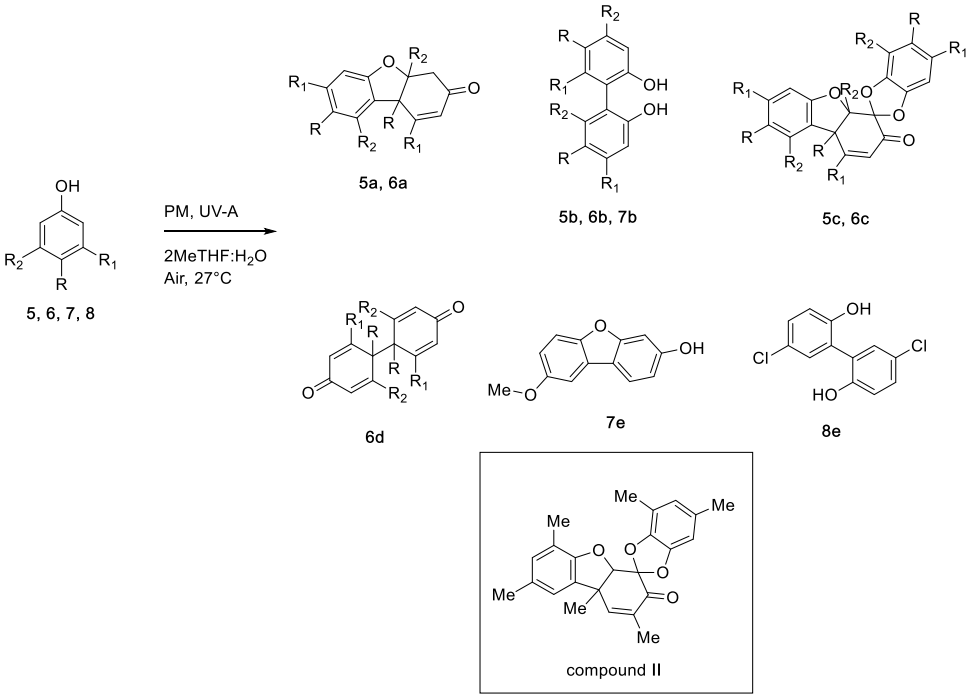

5, 5a, 5b, 5c: R=R_1=Me; R_2=H; 6, 6a, 6b, 6c, 6d: R_1=R_2=H, R=Et; 7, 7b, 7e: R_1=R_2=H, R=O-Me; 8, 8b: R_1=R_2=H, R=Cl

Table 3. Pheomelanin UVA-Driven HRP-Mediated Oxidative Coupling of Substituted Phenols 5−8 in Biphasic Conditions

entry	substrate	R	R1	R2	pH	conversion (%)	product(s)	yield (%)[a]
1	5[b]	Me	Me	H	6	58	**5a(5b)[5c]**	38.6(6.3)[18.1]
2	5[b]	Me	Me	H	7	50	**5a(5b)[5c]**	26.7(3.2)[13.7]
3	5[c]	Me	Me	H	6	43	**5a[5c]**	23.1[9.3]
4	6[b]	Et	H	H	6	70	**6a[6c]⟨6d⟩**	41.4[7.2]⟨6.8⟩
5	6[c]	Et	H	H	6	86	**6a(6b)[6c]⟨6d⟩**	35.4(16.3)[4.3]⟨4.1⟩
6	7[b]	OMe	H	H	6	30	**7b[7e]**	6.12[21.2]
7	8[b]	Cl	H	H	6	60	**8b**	27.2

[a]Yield was calculated based on the amount of the converted substrate. All the reactions were conducted in triplicate. [b]Reaction performed with PM-K. [c]Reaction performed with PM-T.

compound **3** to high polar derivatives not isolated under our experimental conditions,[46] in accordance with data previously reported.[40,47,48] This effect was explained on the basis of the thermodynamic requirement of the successive oxidation of compound **3** in order to complete the single cycle of catalytic turnover of compound **I** (HRP-I) to compound **II** (HRP-II) and native HRP, a process that is operative in the presence of a relatively high amount of the enzyme.[40] In order to optimize the yield of Pummerer's ketone, the reaction was repeated at pH 6 in the presence of 17 units of HRP and different amounts of PM-K (1.0, 0.5, and 0.25% w/w with respect to the substrate). Again, the Pummerer's ketone **2** was isolated as the main reaction product, in addition to dimer **3** and a low amount of 1,1′-dimethyl-[1,1′-bi(cyclohexane)]-2,2′,5,5′-tetraene-4,4′-dione **4** (*para*−*para* dimer) (Scheme 1) in the presence of 1.0 and 0.5% w/w of PM-K (Table 2, entries 4 and 5). The HRP-mediated synthesis of compound **4** was not previously described.[42] Examples of the formation of *para*−*para* dimers by oxidative coupling of phenol derivatives have been reported only in the case of *para*-unsubstituted derivatives, with the only exception of α-cumyl.[49] Note that Pummerer's ketone **2** was obtained in a higher yield at pH 6 than pH 7 (Table 2, entry 4 versus entry 1), confirming the beneficial effect of the acidic medium. pH 6 also favored a high value of the overall mass balance of the reaction. On the other hand, the yield of compound **2**, the conversion of the substrate, and the overall mass balance of the reaction were found to be decreased by decreasing the amount of PM-K (Table 2), highlighting the fundamental role played by pheomelanin in the reaction.[49]

Next, we studied the oxidation of compound **1** with 17 units of HRP and PM-T (1.0, 0.50, and 0.25% w/w) at pH 6. As a general trend, PM-T afforded compound **2** in the conversion of the substrate and with the yield of the product lower than PM-K (Table 2, entries 7−9 versus entries 4−6). Again, the yield of compound **2** and the conversion of the substrate decreased by decreasing the amount of PM-T.

In order to generalize the procedure, the reaction was repeated using a panel of phenols, including 3,4-dimethyl phenol **5**, 4-ethyl phenol **6**, 4-methoxy phenol **7**, and chlorophenol **8**, characterized by substituents with different steric hindrance and stereoelectronic effects. The oxidation of

https://doi.org/10.1021/acsomega.2c06584
ACS Omega 2022, 7, 45688−45696

compound **5** performed at both pH 6 and pH 7 afforded 4a,9b-dihydro-1,7,8,9b-tetramethyl-3(4*H*)-dibenzofuranone **5a** as the main reaction product, in addition to 2,2′-dihydroxy-5,5′-6,6′-tetramethyldiphenyl **5b**, and the spirobenzo[1,3]-dioxol trimer **5c** (Scheme 2 and Table 3, entries 1 and 2). The formation of compound **5c** was unexpected.[39] It showed a structure similar to compound **II** (Scheme 2, highlighted structure) previously isolated after anodic oxidation of 2,4-dimethylphenol.[50] In accordance with these data, compound **5c** was probably formed by successive addition of the phenoxyl radical on the enol form of Pummerer's ketone **5a** followed by monoelectronic transfer and formation of a carbocation intermediate.[50]

When the reaction was repeated in the presence of PM-T at pH 6, compounds **5a** and **5c** were obtained as the only recovered products in the conversion of the substrate and with the yield of the product lower than PM-K (Table 3, entry 3). The oxidative coupling of compound **6** with PM-K at pH 6 afforded 4a,9b-dihydro-8,9b-diethyl-3(4H)-dibenzofuranone **6a** as the main reaction product, in addition to the spirobenzo[1,3]-dioxol trimer derivative **6c** and the *para*−*para* dimer **6d** (Scheme 2 and Table 2, entry 4). In this latter case, the *ortho*−*ortho* dimer was not isolated probably due to the occurrence of oligomerization side processes. Low amounts of compounds **6a**, **6c**, and **6d** were obtained in the presence of PM-T under similar experimental conditions (Table 3, entry 5), with the *ortho*−*ortho* dimer **6b** being detected albeit in a low amount. A different behavior was observed in the oxidation of 4-methoxyphenol **7** with PM-K at pH 6, in which case, 5,5′-dimethoxy-[1,1′-biphenyl]-2,2′-diol **7e** was isolated as the main reaction product, in addition to the *ortho*−*ortho* dimer **7b** (Table 2, entry 6). Probably, the dibenzofuran derivative **7e** was obtained from the corresponding Pummerer's ketone by elimination of MeOH from the adjacent 4a and 9b positions. The oxidation of chlorophenol **8** afforded 5,5′-dichloro-[1,1′-biphenyl]-2,2′-diol **8b** in a low yield and overall mass balance (Table 3, entry 7), probably due to the occurrence of dehalogenation processes.[49,51]

Finally, the oxidation of compounds **1**, **5**, and **6** was studied in monophasic-like conditions by reducing the amount of the buffer in the reaction mixture just to attain the hydration shell of the enzyme.[52] As a general procedure, the selected substrate (0.5 mmol) was dissolved in 2-MeTHF (3.0 mL) in the presence of PM-K (1% w/w) and added with 200 μL of phosphate buffer (0.1 M at pH 6) containing 17 U of HRP followed by irradiation for 48 h at 25 °C. Note that PM-K was solubilized only in part in this system. Under these experimental conditions, the substrates were converted in a lower amount than a previously reported biphasic system to afford desired products in a low yield, suggesting the loss of activity of HRP associated to the low dispersion of PM-K in the reaction medium (Table 4, entries 1−3). In the case of compounds **1** and **5**, the Pummerer's ketones **2** and **5a** were again obtained as the main reaction products, in addition to *ortho*−*ortho* dimers **3** and **5b**, respectively, while compound **6** afforded the *para*−*para* dimer **6d** as the only recovered product. These results confirmed the detrimental effect shown by toluene in the oxidative coupling of compound **1** with HRP and an excess of H_2O_2.[47]

Table 4. Pheomelanin UVA-Driven Oxidative Coupling of Substituted Phenols 1, 5, and 6 in Monophasic Conditions in the Presence of PM-K (1.0% w/w)

entry	substrate	R	R1	R2	conversion (%)	product(s)	yield (%)[a]
1	1	Me	H	H	23	**2**(**3**)	12(2)
2	5	Me	Me	H	34	**5a**(**5b**)	19(5)
3	6	Et	H	H	21	**6d**	6

[a]Yield was calculated based on the amount of the converted substrate. All the reactions were conducted in triplicate.

CONCLUSIONS

We developed a novel photobiocatalytic system in which pheomelanin works as an antenna for the UVA-driven activation of HRP in the oxidative coupling of substituted phenols to yield bioactive Pummerer's ketones. Examples of natural substances bearing the Pummerer's ketone-like tricyclic structure are galantamine, codeine, and usnic acid.[39] In the designed system, singlet oxygen produced by pheomelanin was converted into 2-MeTHF hydroperoxide, while the superoxide anion was dismutated to H_2O_2. PM-K was more efficient than PM-T, probably due to a higher amount of aromatic subunits. The optimal experimental conditions included the use of 1.0% w/w PM-K, 17 U of HRP, and pH 6, in order to facilitate the dismutation of the superoxide anion. The yield of Pummerer's ketone was higher in the biphasic system with respect to the monophasic counterpart, suggesting the partial loss of activity of HRP as a consequence of the reduction of the amount of the buffer, associated to the low solubility shown by pheomelanin in 2-MeTHF. Note that the Pummerer's ketones were obtained in yield and selectivity higher than those of electrochemical, enzymatic, and chemical approaches.[49,50,53−59] Dimers and spirobenzo[1,3]-dioxol trimers were also isolated from the reaction mixture, with the latter compounds being produced by successive addition of the phenoxyl radical on the preformed Pummerer's ketone. The synthesis of trimers from Pummerer's ketones was previously reported only by an electrochemical process.[50] Overall, these results open a new entry for the use of pheomelanin in HRP-mediated photochemical synthetic transformations, avoiding the use of tedious reducing cofactors and the occurrence of undesired and unselective radical side reactions.

EXPERIMENTAL SECTION

Materials and Methods. Horseradish peroxidase (EC 1.11.1.7), reagents, and solvents were obtained from a commercial supplier Merck KGaA, Darmstadt, Germany. UV−visible (UV−vis) spectra were recorded using a Cary 60 UV−vis spectrophotometer, Agilent, Santa Clara, USA. Chemical reactions were monitored using thin-layer chromatography on precoated aluminum silica gel Merck 60 F254 plates, and a UV lamp (λ_{max} = 254 nm) was used for visualization. A Merck silica gel 60 (230−400 mesh) was used for flash chromatography applying the indicated mobile phase. All products were dried in high vacuum (10−3 mbar). ^{1}H NMR and ^{13}C NMR were recorded on a Bruker Avance DRX400 (400 MHz/100 MHz) spectrometer. Chemical shifts for protons and carbons are reported in parts per million (δ scale) and internally referenced to the $CDCl_3$ signal at 7.0 ppm. Coupling constants (J) are reported in Hz. Multiplicities are reported in the conventional form: s = singlet, d = doublet, t = triplet, dd = double of doublets, and m = multiplet. HPLC analysis was performed by an Ultimate 3000 Rapid Resolution UHPLC system (Thermo Fisher Scientific) equipped with an Alltima C18 (250 mm × 4.6 mm, 5 mm) column and a

https://doi.org/10.1021/acsomega.2c06584
ACS Omega 2022, 7, 45688−45696

multiwavelength detector. The UVA apparatus consisted of four lamps (wavelength, 365 nm).

HRP Activity Assay. The enzymatic activity of HRP was determined spectrophotometrically by the pyrogallol assay. The analysis was conducted in a quartz cuvette containing a mixture of pyrogallol (0.8 mmol), phosphate buffer (0.1 M, pH 6), H_2O_2 (30%), and a suitable amount of the enzyme (0.45, 0.67, and 0.75 U/mL). The oxidation of pyrogallol was followed by an absorbance increase at 420 nm. One unit activity of HRP is the amount of the enzyme that transforms 1.0 μmol of pyrogallol per minute at pH 6 and pH 7 at 25 °C.

Evaluation of Enzymatic Activity of HRP in the Presence of PM-K. The enzymatic activity of HRP in the presence of PM-K was determined spectrophotometrically by the pyrogallol assay. The analysis was conducted in a quartz cuvette containing a mixture of pyrogallol (0.8 mmol, 50 mg/mL), phosphate buffer (0.1 M, pH 6), H_2O_2 (30%), PM-K (1% mol), and a suitable amount of the enzyme (0.45, 0.67, and 0.75 U/mL). The oxidation of pyrogallol to obtain purpurgalline was followed by absorbance at 420 nm at 25 °C.

Coumarin Assay. Coumarin (0.2 mmol) was dissolved in 2-MeTHF (4.0 mL); then, 2.0 mL volumes of PBS (0.1 M, pH 6.0) and PM-K/PM-T were added, and the mixture was stirred under UVA irradiation at 25 °C for 48 h under an air atmosphere. At scheduled times (1, 24, and 48 h), the organic phase (100 μL) was picked up and analyzed by a UV−vis spectrophotometer with coumarin and 7-hydroxy-coumarin as references. Results are reported in Figure S8.

General Procedure for the Synthesis of Pummerer's Ketones and Dimers and Derivatives under Biphasic Conditions. Compounds **1** and **5**−**8** (1.0 mmol) were dissolved in 2-MeTHF (5.0 mL) and treated with the appropriate amount of HRP (17, 34, and 68 U) in PBS (5.0 mL) in the presence of PM-K or, in alternative, PM-T (5 mg; 1.0% w/w with respect to the substrate) at the appropriate pH value. The biphasic system was gently stirred (200 rpm) under UVA irradiation and an air atmosphere at 25 °C for 48 h. The organic phase was separated, washed with brine (3 × 4 mL), dried over sodium sulfate, and evaporated under vacuum. The crude product was purified by flash chromatography. The original ^{1}H NMR and ^{13}C NMR spectra of reaction products are reported in the SI.

4a,9b-Dihydro-8,9b-dimethyl-3(4*H*)-dibenzofuranone 2. Oil. Elemental analysis for $C_{14}H_{14}O_2$, expected values: C, 78.48; H, 6.59; O, 14.93; calculated values: C, 78.46; H, 6.59; O, 14.97. MS (EI, 70 eV) m/z 214.10 (100.0%). ^{1}H NMR (400 MHz, $CDCl_3$): δ 7.08 (1H, s, CH), 6.73 (1H, d, J = 8 Hz, CH), 6.47 (2H, m, 2 × CH), 5.94 (1H, d, J = 8.0 Hz, CH), 5.95 (1H, d, J = 10.8 Hz, CH), 4.71 (1H, m, CH), 3.05 (1H, dd, $J1$ = 17.4 Hz, $J2$ = 3.6 Hz, CH_2), 2.80 (1H, dd, $J1$ = 17.4 Hz, $J2$ = 4.0 Hz, CH_2), 2.34 (s, 3H, 2 × CH_3). ^{13}C NMR (100 MHz, $CDCl_3$): δ 190.1, 152.6, 145.6, 126.2, 125.5, 121.7, 119.1, 82.4, 64.4, 40.9, 33.4, 26.7, 25.6.

2,2′-Dihydroxy-5,5′-dimethyldiphenyl 3. Oil. Elemental analysis for $C_{14}H_{14}O_2$, expected values: C, 78.48; H, 6.59; O, 14.93; calculated values: C, 78.48; H, 6.59; O, 14.95. MS (EI, 70 eV) m/z 214.10 (100.0%). ^{1}H NMR (400 MHz, $CDCl_3$): δ 7.13 (2H, dd, $J1$ = 7.6 Hz, $J2$ = 1.6 Hz, CH), 7.04 (2H, s, CH), 6.97 (2H, d, J = 8.0 Hz, CH), 2.33 (6H, s, CH_3). ^{13}C NMR (400 MHz, $CDCl_3$): δ 152.6, 133.4, 131.3, 124.3, 123.0, 118.1, 42.3.

1,1′-Dimethyl-[1,1′-bi(cyclohexane)]-2,2′,5,5′-tetraene-4,4′-dione 4. Oil. Elemental analysis for $C_{14}H_{14}O_2$, expected values: C, 78.48; H, 6.59; O, 14.93; C, 78.43; H, 6.59; O, 14.93. MS (EI, 70 eV) m/z 214.10 (100.0%). ^{1}H NMR (400 MHz, $CDCl_3$): δ 7.01 (4H, d, J = 8.0 Hz), 6.61 (4H, d, J = 8.4 Hz), 2.22 (s, 6H). ^{13}C NMR (100 MHz, $CDCl_3$): δ 182.7, 146.6, 126.3, 40.9, 25.6.

4a,9b-Dihydro-1,7,8,9b-tetramethyl-3(4*H*)-dibenzofuranone 5a. Oil. Elemental analysis for $C_{16}H_{19}O_2$, expected values: C, 79.31; H, 7.49; O, 13.20; calculated values: C, 79.32; H, 7.49; O, 13.21. MS (EI, 70 eV) m/z 243.13 (100.0%). ^{1}H NMR (400 MHz, $CDCl_3$): δ 7.04 (1H, s, CH), 6.65 (1H, s, CH), 5.88 (1H, s, CH), 4.63 (1H, m, CH), 3.05 (1H, dd, $J1$ = 19.6 Hz, $J2$ = 2.0 Hz, CH_2), 2.73 (1H, dd, $J1$ = 21.2 Hz, $J2$ = 3.6 Hz, CH_2), 2.25 (s, 3H), 2.22 (s, 3H, CH_3), 2.25 (s, 3H, CH_3), 1.93 (s, 3H, CH_3), 1.58 (s, 3H, CH_3). ^{13}C NMR (100 MHz, $CDCl_3$): δ 194.7, 158.6, 157.2, 137.8, 129.0, 129.0, 125.9, 125.1, 111.7, 87.8, 47.9, 37.0, 20.5, 20.1, 19.5, 19.5.

4,4′,5,5′-Tetramethyl-[1,1′-biphenyl]-2,2′-diol 5b. Oil. Elemental analysis for $C_{16}H_{18}O_2$, expected values: C, 79.31; H, 7.49; O, 13.20; calculated values: C, 79.31; H, 7.49; O, 13.22. MS (EI, 70 eV) m/z 243.13 (100.0%). ^{1}H NMR (400 MHz, $CDCl_3$): δ 7.02 (2H, s, CH), 6.79 (2H, s, CH), 2.07 (s, 3H, 2 × CH_3), 2.05 (s, 3H, 2 × CH_3). ^{13}C NMR (100 MHz, $CDCl_3$): δ 152.5, 145.4, 126.2, 125.6, 121.7, 119.1, 26.8.

Spirobenzo[1,3]-dioxol Trimer 5c. Oil. Elemental analysis for $C_{24}H_{24}O_4$, expected values: C, 76.57; H, 6.43; O, 17.00; calculated values: C, 76.58; H, 6.43; O, 17.02. MS (EI, 70 eV) m/z 376.17 (100.0%). ^{1}H NMR (400 MHz, $CDCl_3$): δ 7.01 (1H, s, CH), 6.85 (1H, s, CH), 5.91 (1H, s, CH), 5.24 (1H, s, CH), 2.28 (3H, s, 2 × CH_3), 2.24 (3H, s, 2 × CH_3), 1.53 (3H, s, 2 × CH_3). ^{13}C NMR (100 MHz, $CDCl_3$): δ 190.9, 152.5, 145.4, 128.1, 126.9, 126.1, 125.5, 121.6, 119.0, 114.0, 106.0, 103.3, 40.9, 26.8, 25.6.

4a,9b-Dihydro-8,9b-diethyl-3(4*H*)-dibenzofuranone 6a. Oil. Elemental analysis for $C_{16}H_{18}O_2$, expected values: C, 79.31; H, 7.49; O, 13.20; calculated values: C, 79.33; H, 7.49; O, 13.18. MS (EI, 70 eV) m/z 242.13 (100.0%). ^{1}H NMR (400 MHz, $CDCl_3$): δ 7.04−7.01 (3H, m, 2 × CH), 6.74 (1H, d, J = 8.0 Hz, CH), 6.48 (1H, d, J = 8.0 Hz, CH), 6.03 (1H, d, J = 8.0 Hz, CH), 4.86 (1H, m, CH), 3.04 (2H, dd, $J1$ = 15.6 Hz, $J2$ = 4.4 Hz, CH_2), 2.78 (2H, dd, $J1$ = 15.6 Hz, $J2$ = 4.4 Hz, CH_2), 2.63 (2H, m, CH_2), 2.03 (2H, m, CH_2), 1.26 (3H, m, CH_3), 1.06 (3H, m, CH_3). ^{13}C NMR (100 MHz, $CDCl_3$): δ 191.3, 152.6, 145.2, 133.4, 124.3, 123.0, 118.1, 105.8, 80.1, 45.0, 35.0, 24.7, 24.3, 11.8, 5.0.

5,5′-Diethyl-[1,1′-biphenyl]-2,2′-diol 6b. Oil. Elemental analysis for $C_{16}H_{18}O_2$, expected values: C, 79.31; H, 7.49; O, 13.20; calculated values: C, 79.34; H, 7.49; O, 13.14. MS (EI, 70 eV) m/z 242.13 (100.0%). ^{1}H NMR (400 MHz, $CDCl_3$): δ 7.17−7.11 (4H, m, 2 × CH), 6.97 (1H, d, J = 8.0 Hz, CH), 2.65 (4H, q, 2 × CH_2), 1.26 (6H, t, 2 × CH_3). ^{13}C NMR (100 MHz, $CDCl_3$): δ 152.6, 133.4, 127.1, 124.4, 123.0, 118.1, 35.0, 11.9.

Spirobenzo[1,3]-dioxol Trimer 6c. Oil. Elemental analysis for $C_{24}H_{24}O_4$, expected values: C, 76.57; H, 6.43; O, 17.00; calculated values: C, 76.58; H, 6.43; O, 17.05. MS (EI, 70 eV) m/z 376.17 (100.0%). ^{1}H NMR (400 MHz, $CDCl_3$): δ 7.2−7.11 (3H, m, 3 × CH), 6.97−6.80 (3H, m, 3 × CH), 6.74 (1H, s, CH), 5.80 (1H, d, J = 5.2 Hz, CH), 5.44 (1H, s, CH), 2.67−2.53 (6H, m, 3 × CH_2), 1.28−1.26 (9H, m, 3 × CH_3). ^{13}C NMR (100 MHz, $CDCl_3$): δ 190.9, 152.5, 145.4, 128.01, 126.9, 126.1, 125.6, 121.7, 119.0, 114.0, 107.1, 106.0, 103.3, 82.4, 40.9, 33.4, 26.8, 25.6, 18.2.

https://doi.org/10.1021/acsomega.2c06584
ACS Omega 2022, 7, 45688−45696

1,1′-Diethyl-[1,1′-bi(cyclohexane)]-2,2′,5,5′-tetraene-4,4′-dione 6d. Oil. Elemental analysis for $C_{16}H_{18}O_2$, expected values: C, 79.31; H, 7.49; O, 13.20; calculated values: C, 79.31; H, 7.49; O, 13.18. MS (EI, 70 eV) m/z 242.13 (100.0%). ^{1}H NMR (400 MHz, $CDCl_3$): δ 7.09 (2H, d, J = 8 Hz, 2 × CH), 7.79 (2H, d, J = 8 Hz, 2 × CH), 2.60 (4H, q, 2 × CH_2), 1.24 (6H, t, 2 × CH_3). ^{13}C NMR (100 MHz, $CDCl_3$): δ 191.1, 152.7, 123.0, 35.0, 24.3, 11.9.

5,5′-Dimethoxy-[1,1′-biphenyl]-2,2′-diol 7b. Oil. Elemental analysis for $C_{14}H_{14}O_4$, expected values: C, 68.28; H, 5.73; O, 25.99; calculated values: C, 68.29; H, 5.73; O, 26.03. MS (EI, 70 eV) m/z 246.09 (100%). ^{1}H NMR (400 MHz, $CDCl_3$): δ 6.74−6.72 (2H, m, 2 × CH), 6.51 (1H, d, J = 4.3 Hz, CH), 3.78 (3H, s, OCH_3). ^{13}C NMR (100 MHz, $CDCl_3$): δ 145.2, 127.1, 124.4, 123.0, 118.1, 105.9, 45.12.

8-Methoxydibenzo[*b*,*d*]furan-3-ol 7e. Oil. Elemental analysis for $C_{14}H_{14}O_4$, expected values: C, 68.28; H, 5.73; O, 25.99; calculated values: C, 68.29; H, 5.73; O, 26.03. MS (EI, 70 eV) m/z 246.09 (100%). ^{1}H NMR (400 MHz, $CDCl_3$): δ 7.05−6.90 (2H, m, 2 × CH), 6.92 (1H, d, J = 8.8, CH), 6.60 (1H, d, J = 9.2, CH), 6.40 (1H, s, CH), 3.74 (3H, s, OCH_3). ^{13}C NMR (100 MHz, $CDCl_3$): δ 162.8, 158.1, 151.9, 142.1, 136.7, 115.9, 113.3, 104.3, 100.1, 29.5.

5,5′-Dichloro-[1,1′-biphenyl] 8b. Oil. Elemental analysis for $C_{12}H_8Cl_2O_2$, expected values: C, 56.50; H, 3.16; Cl, 27.79; O, 12.54; calculated values: C, 56.50; H, 3.16; Cl, 27.81; O, 12.50. MS (EI, 70 eV) m/z 253.99 (100%). ^{1}H NMR (400 MHz, $CDCl_3$): δ 7.29−7.27 (2H, m, 2 × CH), 6.98 (1H, d, J = 8.8 Hz, CH). ^{13}C NMR (100 MHz, $CDCl_3$): δ 152.7, 129.5, 127.1, 124.4, 123.0, 118.1.

General Procedure for the Synthesis of Pummerer's Ketones and Dimers and Derivatives under Monophasic Conditions. Compounds **1**, **5**, and **6** (0.5 mmol) were dissolved in 2-MeTHF (3.0 mL) and treated with hydrated HRP (17 U, 200 μL) and PM-K/PM-T (5 mg, 1.0% w/w with respect to the substrate) at pH 6. The final mixture was gently stirred (200 rpm) under UVA irradiation and an air atmosphere at 25 °C for 48 h. The organic phase was washed with brine (3 × 4 mL), dried over sodium sulfate, and evaporated under vacuum. The crude product was purified by flash column chromatography.

■ ASSOCIATED CONTENT

Supporting Information

The Supporting Information is available free of charge at https://pubs.acs.org/doi/10.1021/acsomega.2c06584.

Procedures for the synthesis, UV−visible spectra, SEM images, elemental analysis (EDX spectra), electron paramagnetic resonance, UHPLC−MS, FTMS, ESI, and FTIR analyses of the pheomelanin samples; control experiments; evaluation of the concentration of organic hydroperoxide; UV−visible determination of •OH radicals; ^{1}H NMR and ^{13}C NMR spectra (PDF)

■ AUTHOR INFORMATION

Corresponding Author

Raffaele Saladino − *Department of Biological and Ecological Sciences, University of Tuscia, Viterbo 01100, Italy;* orcid.org/0000-0002-4420-9063; Email: saladino@unitus.it

Authors

Sofia Gabellone − *Department of Biological and Ecological Sciences, University of Tuscia, Viterbo 01100, Italy;* orcid.org/0000-0003-1311-3082

Eliana Capecchi − *Department of Biological and Ecological Sciences, University of Tuscia, Viterbo 01100, Italy;* orcid.org/0000-0002-5448-0658

Lucrezia Anastasia Ortelli − *Department of Biological and Ecological Sciences, University of Tuscia, Viterbo 01100, Italy*

Complete contact information is available at: https://pubs.acs.org/10.1021/acsomega.2c06584

Author Contributions

‡S.G. and R.S. contributed equally.

Author Contributions

The manuscript was written through contributions of all authors. All authors have given approval to the final version of the manuscript.

Funding

The PRIN project "ORIGINALE CHEMIAE" in the Antiviral Strategy−Origin and Modernization of Multi-Component Chemistry as a Source of Innovative Broad Spectrum Antiviral Strategy, cod.2017BMK8JR (L.B. and R.S.) is acknowledged.

Notes

The authors declare no competing financial interest.

■ ACKNOWLEDGMENTS

Prof. Rebecca Pogni and Dr. Maria Camilla Baratto, Department of Biotechnology, Chemistry and Pharmacy, Università di Siena, Via A. Moro 2, Siena, 53100 (Italy), are acknowledged for the EPR analyses of pheomelanin samples. CGA (Centro Grandi Apparecchiature, University of Tuscia) is also acknowledged.

■ ABBREVIATIONS

hydrogen peroxide, H_2O_2; 2-methyltetrahydrofuran, 2-MeTHF; horseradish peroxidase, HRP; superoxide dismutase, SOD; 2-methyltetrahydrofuran, 2-MeTHF; *meso*-tetraphenyl porphyrin, *meso*-TPP; pheomelanin from sodium permanganate, PM-K; pheomelanin from mushroom tyrosinase, PM-T; hydroxyl radicals, OH

■ REFERENCES

(1) Napolitano, A.; Memoli, S.; Crescenzi, O.; Prota, G. Oxidative Polymerization of the Pheomelanin Precursor 5-Hydroxy-1,4-benzothiazinylalanine: A New Hint to the Pigment Structure. *J. Org. Chem.* **1996**, *61*, 598−604.

(2) Greco, G.; Panzella, L.; Napolitano, A.; d'Ischia, M. The fundamental building blocks of red human hair pheomelanin are isoquinoline-containing dimers. *Pigm. Cell Melanoma.* **2012**, *25*, 110−112.

(3) Napolitano, A.; Di Donato, P.; Prota, G. Zinc-Catalyzed Oxidation of 5-S-Cysteinyldopa to 2,2′-Bi(2H-1,4-benzothiazine): Tracking the Biosynthetic Pathway of Trichochromes, the Characteristic Pigments of Red Hair *J. Org. Chem.* **2001**, *66*, 6958−6966.

(4) Chatterjee, S.; Prados-Rosales, R.; Itin, B.; Casadevall, A.; Stark, R. E. Solid-state NMR Reveals the Carbon-based Molecular Architecture of Cryptococcus neoformans Fungal Eumelanins in the Cell Wall. *J. Biol. Chem.* **2015**, *290*, 13779−13790.

(5) Gabellone, S.; Piccinino, D.; Filippi, S.; Castrignanò, T.; Zippilli, C.; Del Buono, D.; Saladino, R. Lignin Nanoparticles Deliver Novel

Thymine Biomimetic Photo-Adducts with Antimelanoma Activity. *IJMS* **2022**, *23*, 915.
(6) Tanaka, H.; Yamashita, Y.; Umezawa, K.; Hirobe, T.; Ito, S.; Wakamatsu, K. The Pro-Oxidant Activity of Pheomelanin is Significantly Enhanced by UVA Irradiation: Benzothiazole Moieties Are More Reactive than Benzothiazine Moieties. *IJMS* **2018**, *19*, 2889.
(7) Ou-Yang, H.; Stamatas, G.; Kollias, N. Spectral responses of melanin to ultraviolet A irradiation. *J. Invest Dermatol.* **2004**, *122*, 492−496.
(8) Szewczyk, G.; Zadlo, A.; Sarna, M.; Ito, S.; Wakamatsu, K.; Sarna, T. Aerobic photoreactivity of synthetic eumelanins and pheomelanins: generation of singlet oxygen and superoxide anion. *Pigm. Cell Melanoma Res.* **2016**, *29*, 669−678.
(9) Ito, S.; Kikuta, M.; Koike, S.; Szewczyk, G.; Sarna, M.; Zadlo, A.; Sarna, T.; Wakamatsu, K. Roles of reactive oxygen species in UVA-induced oxidation of 5,6-dihydroxyindole-2-carboxylic acid-melanin as studied by differential spectrophotometric method. *Pigm. Cell Melanoma Res.* **2016**, *29*, 340−351.
(10) Napolitano, A.; Panzella, L.; Leone, L.; d'Ischia, M. Red Hair Benzothiazines and Benzothiazoles: Mutation-Inspired Chemistry in the Quest for Functionality. *Acc. Chem. Res.* **2013**, *46*, 519−528.
(11) Sarna, T.; Sealy, R. C. Free radicals from eumelanins: quantum yields and wavelength dependence. *Arch. Biochem. Biophys.* **1984**, *232*, 574−578.
(12) Ye, T.; Hong, L.; Garguilo, J.; Pawlak, A.; Edwards, G. S.; Nemanich, R. J.; Sarna, T.; Simon, J. D. Photoionization thresholds of melanins obtained from free electron laser-photoelectron emission microscopy, femtosecond transient absorption spectroscopy and electron paramagnetic resonance measurements of oxygen photo-consumption. *Photochem. Photobiol.* **2006**, *82*, 733−737.
(13) Jacobson, E. S. Pathogenic roles for fungal melanins. *Clin. Microbiol.* **2000**, *13*, 708−717.
(14) Nathaniel, C.; Holcomb, R. M. B.; Jarrett, S. G.; Carter, K. M.; Gober, M. K.; D'Orazio, J. A. cAMP-mediated regulation of melanocyte genomic instability: A melanoma-preventive strategy. *Adv. Protein Chem. Struct. Biol.* **2019**, *115*, 247−295.
(15) Panzella, L.; Leone, L.; Greco, G.; D'Errico, G.; Napolitano, A.; d'Ischia, M. Red human hair pheomelanin is a potent pro-oxidant mediating UV-independent contributory mechanisms of melanoma-genesis. *Pigm. Cell Melanoma Res.* **2014**, *27*, 244−252.
(16) Napolitano, A.; Panzella, L.; Monfrecola, G.; d'Ischia, M. Pheomelanin-induced oxidative stress: bright and dark chemistry bridging red hair phenotype and melanoma. *Pigm. Cell Melanoma Res.* **2014**, *27*, 721−733.
(17) Kim, E.; Panzella, L.; Micillo, R.; Bentley, W. E.; Napolitano, A.; Payne, G. F. Reverse Engineering Applied to Red Human Hair Pheomelanin Reveals Redox-Buffering as a Pro-Oxidant Mechanis. *Sci. Rep.* **2015**, *5*, 18447.
(18) Tada, M.; Kohno, M.; Niwano, Y. Scavenging or quenching effect of melanin on superoxide anion and singlet oxygen. *J Clin Biochem Nutr.* **2010**, *46*, 224−228.
(19) Korytowski, W.; Kalyanaraman, B.; Menon, I. A.; Sarna, T.; Sealy, R. C. Reaction of superoxide anions with melanins: electron spin resonance and spin trapping studies. *Biochim. Biophys. Acta, Gen. Subj.* **1986**, *882*, 145−153.
(20) Zippilli, C.; Bizzarri, B. M.; Gabellone, S.; Botta, L.; Saladino, R. Oxidative Coupling of Coumarins by Blue-LED-Driven in situ Activation of Horseradish Peroxidase in a Two-Liquid-Phase System. *ChemCatChem* **2021**, *13*, 4151−4158.
(21) Churakova, E.; Arends, I. W. C. E.; Hollmann, F. Increasing the productivity of peroxidase-catalyzed oxyfunctionalization: a case study on the potential of two-liquid-phase systems. *ChemCatChem* **2013**, *5*, 565−568.
(22) Rauch, M. C. R. F.; Tieves, T.; Paul, C. E.; Arends, I. W. C. E.; Alcalde, M.; Hollmann, F. Peroxygenase-Catalysed Epoxidation of Styrene Derivatives in Neat Reaction Media. *ChemCatChem* **2019**, *11*, 4519−4523.
(23) Hobisch, M.; van Schie, M. M. C. H.; Kim, J.; RøjkjærAndersen, K.; Alcalde, M.; Kourist, R.; Park, C. B.; Hollmann, F.; Kara, S. Solvent-Free Photobiocatalytic Hydroxylation of Cyclohexane. *ChemCatChem* **2020**, *12*, 4009−4013.
(24) Ravanfar, R.; Abbaspourrad, A. The molecular mechanism of the photocatalytic oxidation reactions by horseradish peroxidase in the presence of histidine. *Green Chem.* **2020**, *22*, 6105−6114.
(25) Wang, Y.; Branicky, R.; Noë, A.; Hekimi, S. Superoxide dismutases: Dual roles in controlling ROS damage and regulating ROS signaling. *J. Cell Biol.* **2018**, *217*, 1915−1928.
(26) Hayyan, M.; Hashim, M. A.; AlNashef, I. M. Superoxide Ion: Generation and Chemical Implications. *Chem. Rev.* **2016**, *116*, 3029−3085.
(27) Vianello, A.; Macri, F. Generation of superoxide anion and hydrogen peroxide at the surface of plant cells. *J. Bioenerg. Biomembr.* **1991**, *23*, 409−423.
(28) Cao, W.; Zhou, X.; McCallum, C. N.; Hu, Z.; Zhe Ni, Q.; Kapoor, U.; Heil, C. M.; Cay, K. S.; Zand, T.; Mantanona, A. J.; Jayaraman, A.; Dhinojwala, A.; Deheyn, D. D.; Shawkey, M. D.; Burkart, M. D.; Rinehart, J. D.; Gianneschi, N. C. Unraveling the Structure and Function of Melanin through Synthesis. *J. Am. Chem. Soc.* **2021**, *143*, 2622−2637.
(29) Pyo, J.; Ju, K. Y.; Lee, J. K. Artificial pheomelanin nanoparticles and their photo-sensitization properties. *J. Photochem. Photobiol., A* **2016**, *160*, 330−335.
(30) Ito, S. Optimization of Conditions for Preparing Synthetic Pheomelanin. *Pigm. Cell Melanoma Res.* **1989**, *2*, 53−56.
(31) Al Khatib, A.; Harir, M.; Costa, J.; Baratto, M.C.; Schiavo, I.; Trabalzini, L.; Pollini, S.; Rossolini, G.M.; Basosi, R.; Pogni, R. Spectroscopic Characterization of Natural Melanin from a Streptomyces cyaneofuscatus Strain and Comparison with Melanin Enzymatically Synthesized by Tyrosinase and Laccase. *Molecules.* **2018**, *23*. DOI: 10.3390/molecules23081916
(32) Chance, B.; Maehly, A. C. Assay of Catalase and Peroxidase. *Methods Enzymol.* **1955**, *2*, 764−775.
(33) Shannon, L. M.; Kay, E.; Lew, J. Y. Peroxidase isozymes from horseradish roots. I. Isolation and physical properties. *J. Biol. Chem.* **1966**, *10*, 2166−2172.
(34) Shin, S. K.; Hyeon, J. E.; Joo, Y. C.; Jeong, D. W.; You, S. K.; Han, S. O. Effective melanin degradation by a synergistic laccase-peroxidase enzyme complex for skin whitening and other practical applications. *Int. J. Biol. Macromol.* **2019**, *129*, 181−186.
(35) Okun, M.; Edelstein, L.; Or, N.; Hamada, G.; Donnellan, B. Histochemical studies of conversion of tyrosine and dopa to melanin mediated by mammalian peroxidase. *Life Sci.* **1970**, *9*, 491−505.
(36) Falguera, V.; Moulin, A.; Thevenet, L.; Ibarz, A. Inactivation of Peroxidase by Ultraviolet−Visible Irradiation: Effect of pH and Melanoidin Content. *Food Bioprocess Technol.* **2013**, *6*, 3627−3633.
(37) Monticelli, S.; Castoldi, L.; Murgia, I.; Senatore, R.; Mazzeo, E.; Wackerlig, J.; Urban, E.; Langer, T.; Pace, V. Recent advancements on the use of 2-methyltetrahydrofuran in organometallic chemistry. *Monatsh. Chem.* **2017**, *148*, 37−48.
(38) Ismael, A.; Gevorgyan, A.; Skrydstrup, T.; Bayer, A. Renewable Solvents for Palladium-Catalyzed Carbonylation Reactions. *Org. Process Res. Dev.* **2020**, *24*, 2665−2675.
(39) Sarkar, S.; Ghosh, M. K.; Kalek, M. Synthesis of Pummerer's ketone and its analogs by iodosobenzene-promoted oxidative phenolic coupling. *Tetrahedron Lett.* **2020**, *61*, 152459.
(40) Hewson, W. D.; Dunford, H. B. Oxidation of Horseradish Peroxidase Compound II to Compound I*. *JBC* **1979**, *254*, 3182−3186.
(41) Dobson, G.; Grossweiner, L. Flash photolysis of aqueous phenol and cresols *Trans. Faraday Soc.* **1965**, *61*, 708−714.
(42) Chen, C. L.; Connors, W. J.; Shinker, W. M. Carbonyl compounds from dehydrogenation of p-cresol. *J. Org. Chem.* **1969**, *34*, 2966−2971.
(43) Zhang, J.; Nosaka, Y. Quantitative Detection of OH Radicals for Investigating the Reaction Mechanism of Various Visible-Light

TiO_2 Photocatalysts in Aqueous Suspension. *J. Phys. Chem. C* **2013**, *117*, 1383−1391.
(44) Maier, A. C.; Jonsson, M. Pd-Catalyzed Surface Reactions of Importance in Radiation Induced Dissolution of Spent Nuclear Fuel Involving H_2. *ChemCatChem* **2019**, *11*, 5108−5115.
(45) Leandri, V.; Gardner, J. M.; Jonsson, M. Coumarin as a Quantitative Probe for Hydroxyl Radical Formation in Heterogeneous Photocatalysis. *J. Phys. Chem. C* **2019**, *123*, 6667−6674.
(46) Sahoo, S. K.; Liu, W.; Samuelson, L. A.; Kumar, J.; Cholli, A. L. Biocatalytic Polymerization of p-Cresol: An in-Situ NMR Approach To Understand the Coupling Mechanism. *Macromolecules* **2002**, *35*, 9990−9998.
(47) Pietikäinen, P.; Adlercreutz, P. Influence of the reaction medium on the product distribution of peroxidase-catalysed oxidation of p-cresol. *Appl. Microbiol. Biotechnol.* **1990**, *33*, 455−458.
(48) Çelik, A.; Cullis, P. M.; Lloyd Raven, E. Catalytic Oxidation of p-Cresol by Ascorbate Peroxidase. *Arch. Biochem. Biophys.* **2000**, *373*, 175.
(49) Tanaka, K.; Gotoh, H. Development of the radical C−O coupling reaction of phenols toward the synthesis of natural products comprising a diaryl ether skeleton. *Tetrahedron* **2019**, *75*, 3875−3885.
(50) Malkowsky, I. M.; Rommel, C. E.; Wedeking, K.; Fröhlich, R.; Bergander, K.; Nieger, M.; Quaiser, C.; Griesbach, U.; Pütter, H.; Waldvoge, S. R. Facile and Highly Diastereoselective Formation of a Novel Pentacyclic Scaffold by Direct Anodic Oxidation of 2,4-Dimethylphenol. *EurJOC.* **2006**, *2006*, 241−245.
(51) Dec, J.; Bollag, J. M. Dehalogenation of Chlorinated Phenols during Oxidative Coupling. *Environ. Sci. Technol.* **1994**, *28*, 484−490.
(52) Cortes-Clerget, M.; Yu, J.; Kincaid, J. R. A.; Walde, P.; Gallou, F.; Lipshutz, B. H. Water as the reaction medium in organic chemistry: from our worst enemy to our best friend. *Chem. Sci.* **2021**, *12*, 4237−4266.
(53) Mori, K.; Takahashi, M.; Yamamura, S.; Nishiyama, S. Anodic oxidation of monohalogenated phenols. *Tetrahedron* **2001**, *57*, 5527−5532.
(54) Malkowsky, I. M.; Rommel, C. E.; Fröhlich, R.; Griesbach, U.; Pütter, H.; Waldvogel, S. R. Novel Template-Directed Anodic Phenol-Coupling Reaction. *Chem. − Eur. J.* **2006**, *12*, 7482−7488.
(55) Tzeng, S. C.; Liu, Y. C. Peroxidase-catalyzed synthesis of neolignan and its anti-inflammatory activity. *J. Mol. Catal. B: Enzym.* **2004**, *32*, 7−13.
(56) Hawranik, D. J.; Anderson, K. S.; Simmonds, R.; Sorensen, J. L. The chemoenzymatic synthesis of usnic acid. *Bioorg. Med. Chem. Lett.* **2009**, *19*, 2383−2385.
(57) Navarra, C.; Goodwin, C.; Burton, S.; Danieli, B.; Riva, S. Laccase-mediated oxidation of phenolic derivatives. *J. Mol. Catal. B: Enzym.* **2010**, *65*, 52−57.
(58) Kametani, T.; Ogasawara, K. Studies on the Syntheses of Heterocyclic Compounds. CCXXXVIII. A Modified Synthesis of Pummerer's Ketone. *Chem. Pharm. Bull.* **1968**, *16*, 1138−1139.
(59) Tobinaga, S.; Kotani, E. Intramolecular and intermolecular oxidative coupling reactions by a new iron complex [Fe(DMF)-3Cl2][FeCl4]. *J. Am. Chem. Soc.* **1972**, *94*, 309−310.

https://doi.org/10.1021/acsomega.2c06584
ACS Omega 2022, 7, 45688−45696